Observations of Gradual Solar Energetic Particle Event

2665592K
Astronomy and Astrophysics Group

Sep 2024-Jan 2025

Abstract

Gradual solar energetic particle (SEP) events produce the highest particle intensities at Earth, with particle energies in the range of $\sim 10\,\mathrm{keV}$ up to $\sim 10\,\mathrm{GeV}$. Originating from CME induced shock waves in the inner heliosphere, gradual events accelerate particles via diffusive shock acceleration, a resonant process involving the excitation of Alfvén plasma waves. This gives rise to a power law distribution in particle momentum. Confinement of particles at the shock front by Alfvén waves forms a region behind the shock known as a reservoir where intensities are largely invariant over space and time. Observations of type II solar radio bursts, proton intensities and relative ion abundances associated with gradual events can be used to infer properties such as plasma density, plasma source temperature and spatial and temporal behaviour. Only the most energetic SEPs can be observed on Earth meaning observations made in space play a pivotal role in the study of gradual SEP events. Space-based observations span half a decade from *Skylab* in the 1970s to *Parker Solar Probe* in recent years and planned future missions such as *SunRISE*. Multi-spacecraft observations address challenges involved in observation of gradual events such as large spatial extent and interplanetary scattering, allowing measurements to be compared and correlated in time. Gradual SEP events are an ongoing topic of research as they present a radiation hazard to astronauts and passengers on high-altitude flights and are detrimental to satellite communication and spacecraft electronics. Thus the study of gradual SEP events is crucial in improving our ability to predict and mitigate their effect on human life.

Contents

1 Introduction

1.1 Motivation

Solar energetic particle (SEP) events are defined as enhancements in the intensities of solar particles as a consequence of magnetic activity in the solar atmosphere. Coronal mass ejections, solar flares and solar jets eject electrons, protons and heavier ions into the heliosphere which can be accelerated up to energies in the range of $\sim 10\,\mathrm{keV}$ up to $\sim 10\,\mathrm{GeV}$ in an SEP event (Reames 2021, Whitman et al. 2023). The study of SEP events is critical for the advancement of solar research, vast numbers of energetic particles ejected from the Sun, into the solar system, contain valuable information about magnetic activity in the Sun's upper atmosphere. Observations of SEPs can be used to infer properties of the solar atmosphere, improving our understanding of the physical processes occurring in our nearest star. Further, these observations can be applied to predict the behaviour of SEP events which is vital in mitigating their impact on human operations (Whitman et al., 2023). The high intensities of energetic particles produced by SEP events present a health risk to astronauts and passengers on high altitude flights (Reames, 2013). In addition to creating a health-risk to humans, SEPs cause issues for satellite technologies and can alter the Earth's atmosphere and local magnetic field in the form of geomagnetic storms (Desai & Giacalone, 2016). For these reasons, SEP events are an ongoing topic of research.

1.2 SEP Events

Convective energy transport and differential rotation in the outer layer of the Sun create motion in the solar plasma. This plasma motion creates a continually changing magnetic field, giving rise to the magnetic activity, e.g. flares and coronal mass ejections, which precedes solar energetic particle events (Reames, 2021). Coronal mass ejections, associated with gradual events, are large eruptions of solar plasma from the solar atmosphere, arising from the transition of the coronal magnetic field from a high energy configuration to a low energy configuration by a process called magnetic reconnection (Reid 2011, Reames 2021). CMEs have large angular extent and extend from the solar surface all the way out to interplanetary space (Chen, 2011). Eruptions caused by CMEs contain masses between $10^{14}\,\mathrm{g}$ and $10^{16}\,\mathrm{g}$ with kinetic energies in the range 10^{27}–$10^{32}\,\mathrm{ergs}$ (Reames, 2021). Associated with impulsive events, flares and jet also arise from magnetic reconnection but are significantly more localised than CMEs with angular extents below 30° (Desai & Giacalone, 2016).

SEP events are broadly categorised as gradual or impulsive, corresponding to their relative duration. Impulsive events last on the order of hours and gradual events last on the order of days (Desai & Giacalone, 2016). Both types of event arise due to solar magnetic phenomena- gradual events are associated with shock waves produced by fast coronal mass ejections (CMEs) and impulsive events with solar flares and solar jets (Reames, 2013). Of the two categories, gradual events produce the highest energetic particle intensities and therefore pose the greatest radiation risk and cause the majority of space-weather effects (Desai & Giacalone, 2016).

While CMEs and solar flares/jets are distinct solar phenomena they often take place at the same time with e.g. solar flares contributing to the coronal mass ejection particle population (Tylka et al., 2001). Thus gradual and impulsive events are often observed to occur together, historically making it difficult to identify the correct origin of a given SEP event (Desai & Giacalone, 2016).

1.3 Observation

Observation of SEP events is typically undertaken in space as the Earth's magnetic field prevents the majority of SEPs from reaching the ground for ground-based observations. The Earth's atmosphere is opaque to radiation outside of visible and radio wavelengths thus observations of more energetic electromagnetic radiation such as x-rays and γ rays must also be made in space. Measurable properties of gradual events include proton intensities and relative ion abundances which are observed using *in situ* instruments on-board spacecraft (Reames, 2013). Measurements are used to investigate acceleration mechanisms, CME shock properties and infer coronal and photospheric composition. Space-based observations were key in the delineation of SEP events into two different classes (Desai & Giacalone, 2016). Specifically, space-based observations were used to disprove the idea, known as the 'solar flare myth' (Gosling, 1993), that solar flares were the sole cause of SEP events and their associated geomagnetic phenomena by taking measurements at different locations relative to the Sun with multiple spacecraft (Desai & Giacalone, 2016).

Multi-craft observations spatially resolve gradual events in a way which cannot be afforded by observing from one location alone, providing comparisons between different positions which are used to explore the spatial and temporal behaviour of these large events (Reames, 2013). Additionally, multi-craft observations address some of the challenges involved in observing gradual SEP events. Currently *Parker Solar Probe* is collecting data in the near-Sun environment, delivering measurements in regions of the heliosphere where interplanetary scattering and other transport phenomena have a smaller effect on particle properties (Desai & Giacalone, 2016). These measurements, combined with those made closer to Earth, allow for the identification of the individual physical processes at play in gradual SEP events, separating interplanetary scattering from other phenomena (Desai & Giacalone, 2016). *Parker Solar Probe* continues to make measurements during the solar maximum time period as it nears the end of its primary mission. In the near future, *SunRISE* is planned to launch, aiming to image low frequency solar radio bursts using multiple craft as an aperture synthesis interferometer with minimal on-board processing (Lazio et al., 2022).

While the majority of observations require space-based measurements, there are some properties of gradual SEP events which can be observed on the ground. Type II solar radio bursts emitted by electrons in SEP events via the plasma emission mechanism can be observed on the ground and used to measure plasma electron density (Bastian et al., 1998). The most energetic gradual events can accelerate particles to high enough energies to penetrate the Earth's atmosphere in a ground level enhancement (GLE) which can be observed on the ground (Forbush, 1946).

This review will cover observations of gradual SEP events by describing some of the physical characteristics of gradual SEP events and the key properties which can be observed to learn more about these phenomena. Space-based observations will be review with a particular focus on those made using multiple spacecraft and how various observational challenges are addressed. Finally, details of recent and future developments in observations of gradual SEP events will be discussed.

2 Gradual SEP Events

2.1 Origin

Gradual SEP events are initiated by large ejections of plasma material from the Sun's upper atmosphere into the heliosphere known as coronal mass ejections (Reames, 2013). CMEs occur when a region of coronal magnetic field undergoes a transition from a high energy configuration to a lower energy configuration via magnetic reconnection. This change in topology, and therefore energy, of the magnetic field releases energy by accelerating particles to high enough energies to be ejected into the heliosphere (Reames, 2021). If the CME is moving at a speed greater than the speed at which magnetic waves propagate in the plasma, known as the local Alfvén speed, a shock wave will be formed (Reames, 2013). The local Alfvén speed is given by

$$v_{\mathrm{A}} = \frac{B}{\sqrt{\mu_0 \rho}}, \tag{1}$$

where B is the local magnetic field strength, μ_0 is the permeability of free-space and ρ is the plasma density (Kim et al., 2018). The shock wave produced expands out into the heliosphere, accelerating ejecta via a process called diffusive shock acceleration.

2.2 Diffusive Shock Acceleration

The shock produced by a fast CME is responsible for accelerating the particles involved in a gradual SEP event via diffusive shock acceleration (DSA). Particle pitch, also known as pitch angle cosine, μ, is the angle between the particle momentum vector, $\mathbf{p}$, and the local magnetic field vector, $\mathbf{B}$, given by

$$\mu = \frac{\mathbf{p} \cdot \mathbf{B}}{pB}, \tag{2}$$

(Drury, 1983). In DSA, magnetic interactions lead particles to change direction via pitch-angle scattering, crossing back and forth across the shock front in a resonant process (Reames, 2021). With each round-trip across the shock, particles are accelerated to higher energies, exciting Alfvén plasma waves as they stream away from the shock (Reames, 2013). These Alfvén waves are produced with wave-number, k, given by

$$k = \frac{B}{\mu P}, \tag{3}$$

where B is the magnetic field strength, μ is the scattering pitch angle cosine, as above, and P is the particle rigidity, defined as the ratio of the particle momentum to charge (Reames, 2004). Different particle rigidities, P, due to different charges, masses and velocities of protons, electrons and heavier ions result different Alfvén wave wave-numbers, creating a spectrum of Alfvén waves (Reames, 2004). Differences in rigidity between particle species cause different scattering effects which can be inferred by observing particle abundance ratios and angular distributions, allowing the Alfvén wave spectrum to be investigated (Reames 2004, Ng et al. 1999).

Excited Alfvén waves create magnetic turbulence which increases SEP scattering effects, scattering particles to higher energies and trapping them closer to the shock. Particles trapped at the shock are accelerated more efficiently and climb to higher and higher energies,

exciting more Alfvén waves resonant with this higher energy, further increasing scattering effects (Reames, 2004). Confinement of particles at the shock front by Alfvén waves limits the flow of particles away from the shock. This creates a streaming limit which places an upper limit on the intensity of particles streaming away from the shock front (Reames 2021, Reames 2013).

Diffusive shock acceleration produces a power law particle distribution, f, in particle momentum, p, where the power depends solely on the compression ratio of the shock, R, (Reames 2021, Drury 1983, Cristofari et al. 2022),

$$f\left(p\right) \propto p^{-3R/(R-1)}, \tag{4}$$

where R is defined as the ratio of the upstream plasma velocity to the downstream plasma velocity (Reames, 1999). R can also be related to the plasma specific heat ratio, γ, and the shock Mach number, M, by

$$R = \frac{\gamma + 1}{\gamma - 1 + M^{-2}}, \tag{5}$$

which for a strong, non-relativistic, shock, with $M \gg 1$ and $\gamma = \frac{5}{3}$, gives a spectrum $f\left(p\right) \propto p^{-4}$. This gives approximately the same power law index obtained from observations of galactic cosmic ray spectra, suggesting DSA as a potential acceleration mechanism for galactic cosmic rays (Cristofari et al. 2022, Drury 1983).

2.3 Characteristics

Since particles move back and forth across the shock as part of the DSA process, the shock is largely collision-less meaning energy is transferred between particles electromagnetically (Desai & Giacalone 2016, Drury 1983). Due to this electromagnetic interaction between particles, the thickness of the shock is approximately given by the gyroradius of an ion in the plasma (Drury, 1983). A particles gyroradius is the radius of its circular or helical orbit around a magnetic field line and is given by

$$r_{\mathrm{g}} = \frac{p_{\perp}}{ZeB}, \tag{6}$$

where m is the particle mass, Z is the particle atomic number, e is the elementary charge and $p_{\perp}$ is the particle momentum component perpendicular to the magnetic field B (Drury, 1983). Equation 6 implicitly contains a particle mass to charge ratio term, included in the perpendicular momentum, $p_{\perp}$, component divided by particle charge, Ze. According to Desai & Giacalone (2016), particles with lower mass to charge ratios are accelerated more efficiently by diffusive shock acceleration, because a lower mass to charge ratio gives a smaller gyroradius, allowing particles to be successfully confined to the shock front where acceleration is most efficient.

Efficient entrapment of particles at the shock front throttles particle motion away from the shock. Throttling of particles near the shock results in the formation of a region behind the shock known as a 'reservoir' where particles are unable to escape, causing intensities to be largely invariant in space and time (Reames 2013, Desai & Giacalone 2016). This particle reservoir is responsible for the 'gradual' decay of particle intensities characteristic of gradual SEP events. Particles trapped in a reservoir are also available for acceleration by a subsequent CME, providing a 'seed' population (Reames, 2013).

Gradual events are distributed widely in solar longitude. SEPs from gradual events occupy a broad width of heliospheric magnetic field lines as they propagate from the solar surface through the heliosphere, with the accompanying CME covering between 100° and 200° in solar longitude (Desai & Giacalone, 2016). This can pose a challenge when it comes to observing gradual events from one location (Reames, 2013), as discussed in section 4.

2.4 Impact

Since they produce the highest SEP intensities, gradual events create a larger risk to human operations than their impulsive counterpart (Desai & Giacalone, 2016). Increased radiation exposure poses a health risk to astronauts particularly those outside of the Earth's magnetic field. This is especially important for manned-missions to the Moon and potential future missions to Mars where there are uncertainties in predicting the impact that SEPs produced by gradual events outside of low Earth orbit, specifically heavier ions, will have on astronaut health (Cucinotta et al. 2010, Cucinotta et al. 2021, Kim et al. 2011).

SEPs can also damage space-craft materials and on-board electronics. Ionisation from energetic particles can, potentially irreversibly, damage semi-conductor materials inside micro electronics components (Stassinopoulos & LaBel, 2004). Protons energies between 0.1 MeV and 10 MeV cause surface damage to spacecraft materials with protons in the upper limit of this range having sufficient energy to damage craft solar cells. Additionally, changes to local magnetic fields can interfere with satellite navigation systems and induce currents in electronic devices (Iucci et al., 2005).

The most energetic gradual SEP events can accelerate protons to energies of order GeV. These protons, associated with very fast CMEs moving at $\sim$ 2000 km s^{-1}, are energetic enough to infiltrate Earth's atmosphere, causing what is known as a ground level enhancement (GLE) (Gopalswamy et al., 2012). The highly energetic nature of these events can cause changes in the Earth's atmosphere and magnetic field. SEPs in a ground-level enhancement have sufficient energy to reach the lower atmosphere and can cause permanent ionisation of the surrounding air (Usoskin et al., 2011). Energetic particles produced in a GLE can also cause alterations to the Earth's magnetic field in phenomena known as geomagnetic storms (Gonzalez et al., 1994). Alterations made to the Earth's environment in this way can have a serious impact on human life with a famous example being the geomagnetic storm on March 13th 1989 which heavily affected power systems in Canada (Boteler, 2019).

3 Observables

As detailed by Reames (2002), high intensities and long durations make gradual SEP events easier to observe than impulsive events. Measurements of solar radio bursts, proton intensities and ion abundance ratios provide valuable insight into the nature of gradual events.

3.1 Type II Solar Radio Bursts

Solar radio bursts emitted by accelerated electrons are used to investigate the properties of SEP events. There are five types of solar radio burst, with Type II and type III bursts being of particular interest in the study of SEP events (Reid, 2011). Type II bursts correspond to gradual events while type III events are associated with impulsive events (Reames, 2013).

The classification of these radio bursts into types is based on their frequency drift, $d\nu/dt$, and was first established by Wild & McCready (1950) by using an aerial to receive high intensity radio signals emitted by the Sun on the ground. Type II bursts have a slow frequency drift $\approx -0.25\,\mathrm{MHz\,s^{-1}}$ in comparison to the faster drifting type III bursts with a frequency drift of $\approx -20\,\mathrm{MHz\,s^{-1}}$ (Melrose, 2017).

The plasma emission mechanism, initiated by an electron streaming instability, results in the emission of type II solar radio bursts in the case of gradual SEP events (Reid, 2011). Type II radio burst emission by the plasma emission mechanism is partly circularly polarised and occurs at two frequencies, the fundamental plasma frequency ν_{pe}, known as F emission, and the second harmonic at $2\nu_{\mathrm{pe}}$, known as H emission (Reid 2011, Melrose 2017, Bastian et al. 1998). The mechanism occurs in three stages with the first being the excitation of Langmuir waves by the electron beam instability. This beam instability arises from fast electrons overtaking slower electrons in the electron beam, corresponding to a point in space, described by position vector $\mathbf{x}$, with a positive slope of the electron distribution function, $f(\mathbf{x},\mathbf{v},t)$ [electrons $\mathrm{cm^{-4}\,s}$] in velocity space, described by $\mathbf{v}$ (Reid, 2011). Here, $\partial f(\mathbf{x},\mathbf{v},t)/\partial \mathbf{v} > 0$ implies there is a higher density of faster electrons at this position compared to other parts of the beam (Reid, 2011). The electron distribution function has the following properties,

$$n(\mathbf{x},t) = \int f(\mathbf{x},\mathbf{v},t)\,d^3\mathbf{v}, \quad N(t) = \int n(\mathbf{x},t)\,d^3\mathbf{x}, \tag{7}$$

where $n(\mathbf{x},t)$ is the electron number density at position $\mathbf{x}$ at time t and $N(t)$ is the total number of electrons at time t. This distribution function allows modelling of plasma particle-particle interactions of a large group of particles without simulating individual particle interactions (Reid, 2011).

An unstable electron beam configuration ($\partial f(\mathbf{x},\mathbf{v},t)/\partial \mathbf{v} > 0$) induces Langmuir waves in the plasma which contribute to the second stage of the plasma emission mechanism. The second stage involves emission at the fundamental (F) frequency via induced scattering of Langmuir waves off thermal ions. According to Reid (2011), this process is similar to Thomson scattering except, instead of a free electron, it's the shielding effect of the electron cloud surrounding the ion which scatters the incident Langmuir wave. F emission can also occur via the coalescence or decay of Langmuir waves with ion sound waves. Second harmonic (H) emission occurs solely from the superposition of two Langmuir waves travelling in opposite directions (Reid 2011, Melrose 2017).

Emission at the two plasma frequency harmonics give radio signals produced by the plasma emission mechanism a unique two-band structure in frequency which can be used to distinguish them from other radio sources (Desai & Giacalone, 2016). Measurements of radio burst frequency against time are plotted on dynamic spectra with burst intensity relative to background given by contour colours as displayed in figure 1 (Reid 2011, Desai & Giacalone 2016). The cyan lines in figure 1 denote the frequency bands which comprise the burst, allowing the frequency drift to be calculated. In this particular observation, the burst was found to have a frequency drift of $\sim -0.2\,\mathrm{MHz\,s^{-1}}$ (Kumari et al., 2023).

The fundamental plasma frequency is given by

$$\nu_{\mathrm{pe}}\,[\mathrm{MHz}] = \sqrt{\frac{e^2 n_{\mathrm{e}}}{\pi m_{\mathrm{e}}}} \times 10^{-6} \approx 9 \times 10^{-3}\sqrt{n_{\mathrm{e}}}, \tag{8}$$

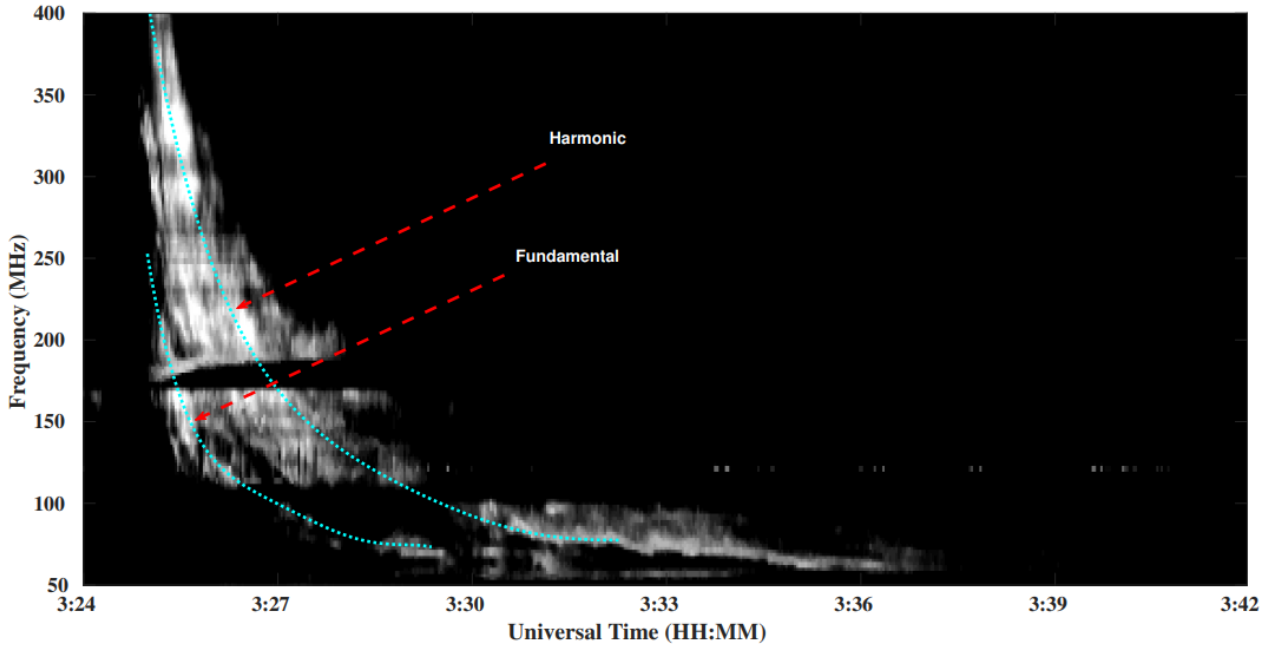

Figure 1: Dynamic spectra of a type II solar radio burst. Taken using the CALLISTO spectrometer at the ground-based Gauribidanur Radio Observatory on November 4 2015 (Kumari et al., 2023).

where e is electron charge, m_e is the electron mass and n_e is the plasma electron number density (Bastian et al., 1998). Thus, using observations of solar radio bursts, the electron number density profile of a radio burst emitting plasma can be traced out (Bastian et al., 1998). The relation between fundamental plasma frequency and plasma electron density in (8) explains why gradual events are associated with slow drifting type II bursts while impulsive events are associated with fast drifting type III bursts. Due to the localised nature of impulsive events, electron number density falls off sharply with distance from the Sun, corresponding to the fast radio burst frequency drift associated with impulsive SEP events. Oppositely, gradual events have large spatial extent and sustain electron densities farther from the Sun resulting in a slower frequency drift (Reames, 2021).

3.2 Proton Intensities

Due to their low mass to charge ratio, DSA accelerates protons more efficiently than other SEP species, making protons the most abundant particle in gradual SEP events (Desai & Giacalone 2016, Reames 2004). Observations of proton intensities convey gradual event spatial and temporal behaviour, allowing acceleration mechanisms and radiation hazards to be better understood (Desai & Giacalone, 2016).

Kahler (2001) investigated the relation between CME shock speed using data collected by Wind/EPACT/LEMT, SOHO/LASCO, Helios and Solwind. Figure 2 shows correlations between peak proton intensity and CME shock speed at two different energies (Kahler 2001, Desai & Giacalone 2016). The large variations in peak proton intensity with CME shock speed indicate that other variables, such as the streaming limit, affect peak proton intensity. Variations also occur due to observed peak intensity and CME shock speed being heavily depend on observer solar longitude (Reames, 2013). In spite of this, the general trend is that peak proton intensity increases with increasing CME shock speed (Reames, 2013).

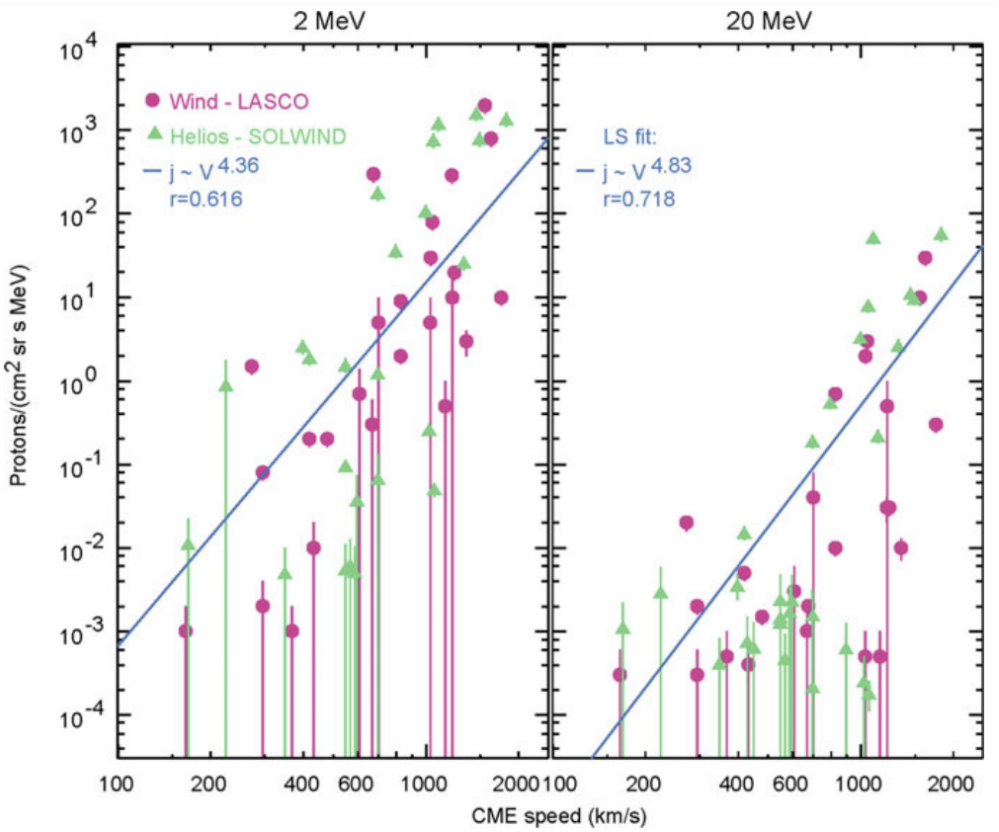

Figure 2: Peak proton intensity against CME speed for two different proton energies. Pink circles denote measurements made by Wind/EPACT/LEMT and SOHO/LASCO. Green triangles indicate data from Helios and Solwind. Blue lines show the linear least-square fits to each dataset with correlation coefficient given by r (Desai & Giacalone, 2016).

Measurements of proton intensities reveal the temporal behaviour of gradual SEP events. Proton intensities with time at different energies are presented in figure 3, excellently illustrating the four different stages of a gradual SEP event, onset, plateau, shock and reservoir/decay stage, which are labelled along the base of the plot (Reames, 2013). The plateau stage corresponds to the streaming limit placing an upper bound on particle intensities streaming away from the shock as detailed in section 2.2. Peak intensities are observed at the time of shock passage at the observer and the reservoir/decay stage begins as the observer enters the reservoir region behind the shock (Reames, 2004). Invariant intensities during the reservoir/decay stage suggest that very few particles are able to escape the particle reservoir (Desai & Giacalone, 2016). Additionally, protons represented by figure 3 follow the power law particle distribution associated with DSA, with higher intensities of lower energy protons and lower intensities of higher energy protons.

3.3 Relative Ion Abundances

Measurements of ion abundances played a key role in making the distinction between the two classes of SEP event (Reames, 2021). Gradual events usually have the same relative ion abundances as the local coronal plasma values at temperatures between 1 MK and 2 MK (Reames, 2004). Impulsive events, however, are characterised by a three order of magnitude enhancement of the ratio of ^{3}He to ^{4}He relative to solar wind values with heavier elements receiving

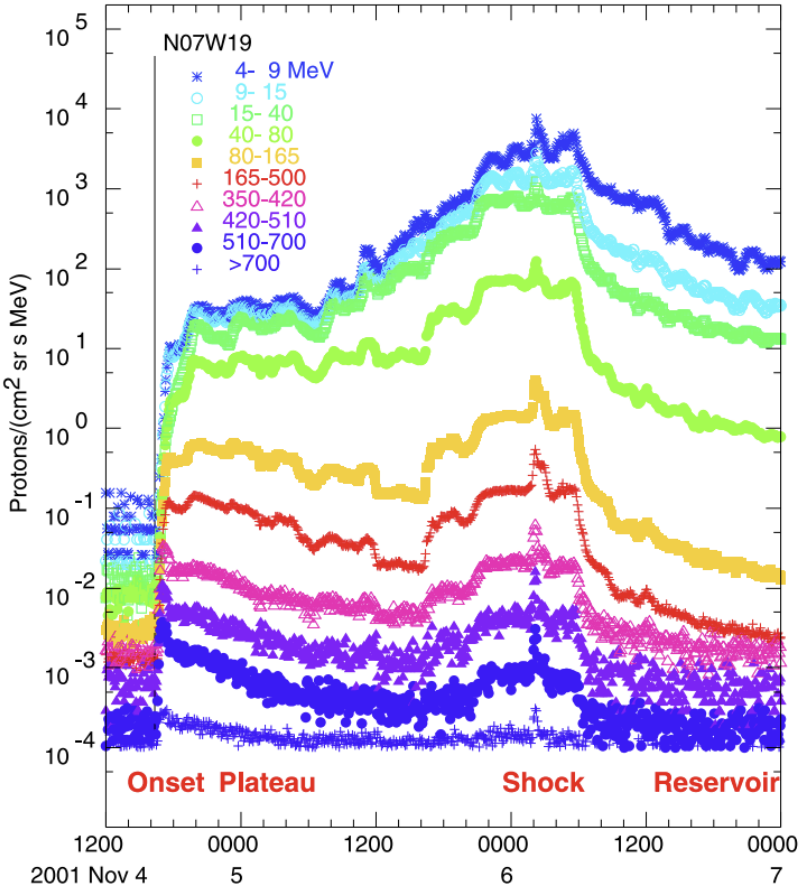

Figure 3: Proton intensities measured at various energies by the NOAA/GOES network on November 4 2001 Reames (2013).

similar order of magnitude enhancements in their ratio to He or O (Reames, 2021). In addition to distinguishing between gradual and impulsive SEP events, measurements of relative abundances have demonstrated the difference between the solar wind and SEPs. Comparisons of relative ion abundances corresponding to SEP events and different background solar wind speeds made by Kahler et al. (2009) showed no change in SEP composition with variations in background solar wind speed, implying SEPs and the solar wind are separate phenomena with different physical origins (Desai & Giacalone, 2016).

As outlined in subsection 2.3, particle mass to charge ratio influences scattering by Alfvén waves meaning particles with low mass to charge ratios are transported more effectively (Desai & Giacalone, 2016). This affects which species are observed and their corresponding abundance ratios. Particles with different rigidities, P, resonant with different Alfvén wavenumbers meaning measurements of abundances can be used to investigate the Alfvén wave spectrum produced by the shock in a gradual SEP event (Reames, 2004). Mass to charge ratio depends on the first ionisation potential (FIP) ie the energy required to remove one electron from the outer shell of a neutral atom. Elements with FIP less than 10 eV are ionised in the photosphere and easily dragged out into the corona by Alfvén waves (Reames 2021, Laming 2009). This property of Alfvén waves alters the coronal abundances relative to those in the photosphere, causing ions to be 3–4 times more abundant in the corona compared to in the photosphere while species in the corona with FIP greater than 10 eV follow photospheric abundances (Laming, 2009). This discrepancy between abundances of ions and neutral ions in the photosphere and corona can be used to determine particle origin in the solar atmo-

sphere.

Ion abundances can also be used to infer plasma source temperature by using the dependence of an ions mass to charge ratio, A/Q, on temperature, T (Reames, 2016). Plots of theoretical A/Q with temperature are compared to average relative abundance values in a given time interval to determine the source temperature, as shown in figure 4. This method relies on the fact that there is a power law relation between a species' relative abundance and its mass to charge ratio, A/Q, causing trends in A/Q to be reproduced in trends in abundance enhancements. In figure 4, the temperature at which the enhancements of elemental abundances with atomic number between those of He and Fe follow the same trend as their corresponding mass to charge ratios is ~ 1 MK (Reames, 2016).

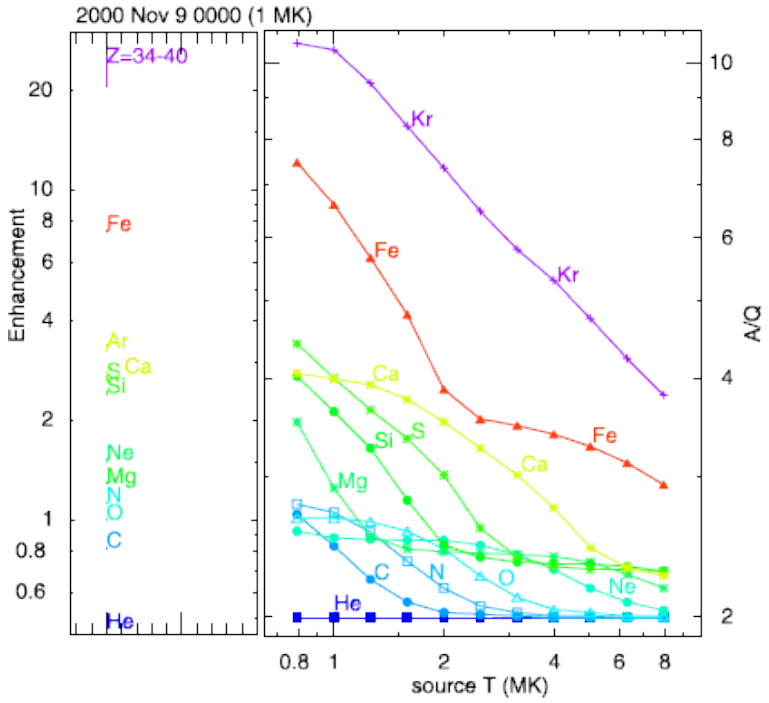

Figure 4: *Left-panel*: Enhancements in elemental abundances relative to oxygen at 3–5 MeV amu^{-1}, normalised to coronal values. This means enhancements plotted in the left-panel are actually Z/O/(coronal value), where Z is some element, as opposed to just Z/O. *Right-panel*: Theoretical mass to charge ratio, A/Q, of assorted elements against temperature, T. Data taken between 0000 and 0800 UT on November 9th 2000 (Reames, 2016).

3.4 Ground Level Enhancements (GLEs)

Similar to type II radio bursts, GLEs can be observed on Earth as the high particle energies involved allow penetration of the Earth's atmosphere and detection on the ground. Ground level enhancements are detected by neutron monitors, muon detectors and ionisation chambers, designed to detect galactic cosmic rays, when incident high energy SEP event protons produce nuclear cascades in the upper atmosphere, enhancing cosmic ray intensities above background levels (Desai & Giacalone 2016, Reames 2013). The first observed SEP events were GLEs and were observed by Forbush (1946) using an ionisation chamber. Forbush recorded three increases in cosmic ray intensities, shown in figure 5, which all coincided with a visible solar flare and a corresponding radio fade-out suggesting a relation between solar magnetic activity and energetic particles arriving at Earth. Based on the particle energies

required to cause a GLE, Forbush likely saw an increase in cosmic ray intensity as a result of the combination of a gradual event and the impulsive event associated with the visible flare in a large SEP event. Rather than a single impulsive event (Desai & Giacalone, 2016). These preliminary observations of GLEs gave rise to the field of SEP research (Cliver, 2008).

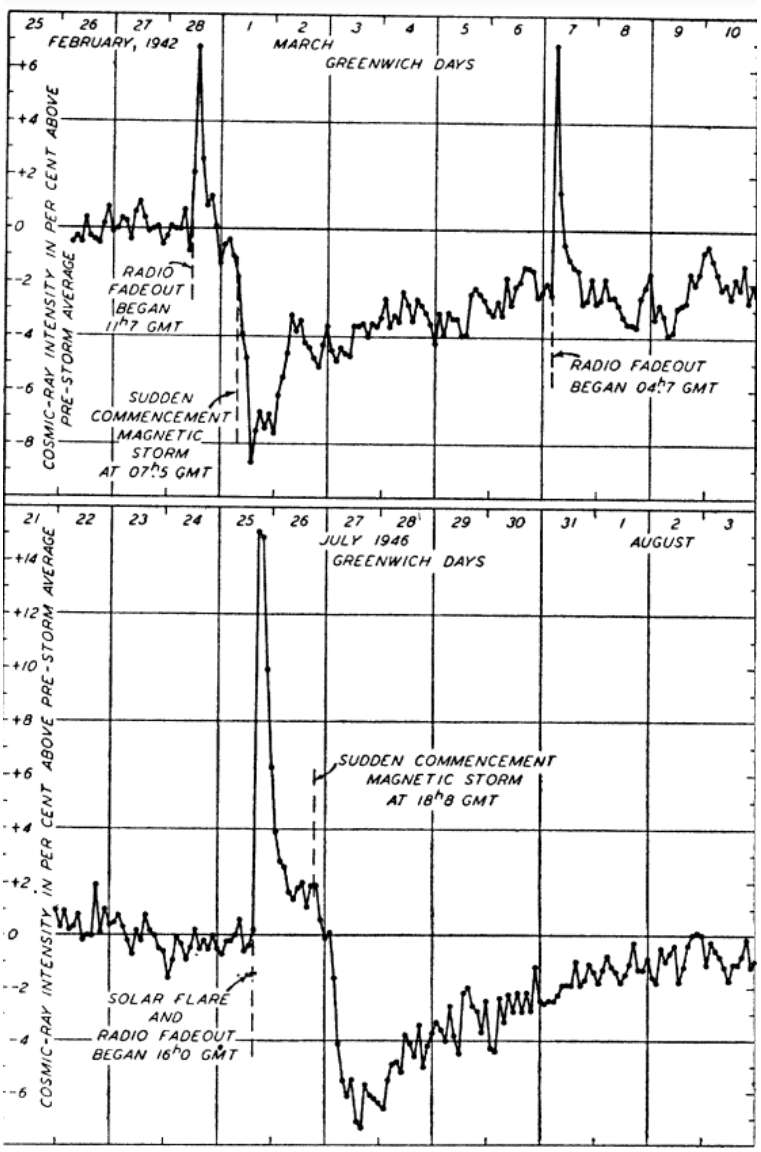

Figure 5: Cosmic ray intensities observed in Cheltenham, Maryland by Forbush (1946) between February 25th and March 10th 1942 and July 21st and August 3rd 1946.

4 Space-based Observations

4.1 Key Spacecraft

The advent of space-based observations allowed for a fuller examination of gradual SEP events in the absence of the shielding effect of the Earth's magnetic field and atmosphere. Early space-based observations include those made by *Skylab*, launched in 1970s as NASA's first space station, which linked CMEs and so-called 'large proton events', leading to important developments in the two-class picture of SEP events (Desai & Giacalone, 2016).

Helios 1 and 2, launched in 1974 and 1976, respectively, investigated the inner heliosphere, providing measurements of proton intensities which could be compared to those made by spacecraft further out in the Solar System such as *Voyager* 2 (Desai & Giacalone 2016, Reames 2023). Similar to the *Helios* craft, *Ulysses*, launched in 1990, investigated the composition of SEPs and solar wind particles and discovered the reversal of the solar magnetic field every 11 years as part of the solar cycle. *Ulysses* followed a highly eccentric orbit probing the inner heliosphere at perihelion and reached Jupiter at ~ 5 AU at aphelion. In conjunction with *IMP* 8, *Ulysses* observed uniform reservoir intensities spanning over 2.5 AU (Reames, 2023).

The *WIND* craft was launched in 1994 to investigate interactions between the solar wind and the Earth's magnetic field and atmosphere. *WIND* carried the *WAVES* instrument, designed to measure radio and plasma waves with frequencies in the range of ~ 0.1 Hz up to 14 MHz and 3 kHz for the electric and magnetic field components, respectively (Bougeret et al., 1995). Measurements made by *WIND/WAVES* produced a catalogue of observations type II radio bursts which were then used to estimate shock speed and study the temporal behaviour of interplanetary shocks (Gopalswamy et al., 2019).

SOHO, launched in 1995, orbited the Sun-Earth system at the $L1$ Lagrangian point and observed particles over a wide range of energies from 44 keV to 53 GeV per nucleon (Bothmer et al., 1997). *SOHO* measured CME speed and size and investigates the connection between these properties and peak proton intensity. Every SEP event, even impulsive events, observed by *SOHO* were accompanied by a CME as measurements were taken during solar minimum when flares likely have insufficient energy to cause an impulsive event on their own (Bothmer et al., 1997).

Lastly, *STEREO A* and *B* were launched in 2006 with one craft ahead of Earth in its orbit and the other behind in order to document the full extent of large gradual SEP events (Reames, 2023). The two craft were used to discover that CME shocks can wrap around the Sun, crossing multiple magnetic field lines. The *STEREO* craft also played a role in declaring diffusive shock acceleration as the prevailing theory of SEP acceleration in gradual SEP events (Reames, 2023).[1]

4.2 Multi-spacecraft Observations

Due to their large spatial extent, observations of properties of gradual SEP events are highly dependent on observer solar longitude (Reames, 2013). Cane et al. (1988) analysed the longitude dependent behaviour of the intensity-time profiles of 235 gradual SEP events over the course of $\sim$ 20 years using data from *IMP*s 4 to 8 and *ISEE* 3, ordering them based on observer solar longitude. Figure 6 presents the results of this analysis, displaying typical intensity profiles at a given observer longitude (Desai & Giacalone, 2016). Intensity profiles vary with position and observer magnetic connectivity, with some intensities unexpectedly peaking when the observer is behind the shock, due to increased magnetic connectivity connecting the observer to the shock nose from behind (Reames, 2021). At each of the three locations, peak intensity is recorded at the time of shock passage at the observer.

Using multiple spacecraft alleviates the longitude-dependence of observations, probing the

[1]Uncredited information about NASA missions was obtained from the respective mission web-pages at *https://science.nasa.gov/missions* .

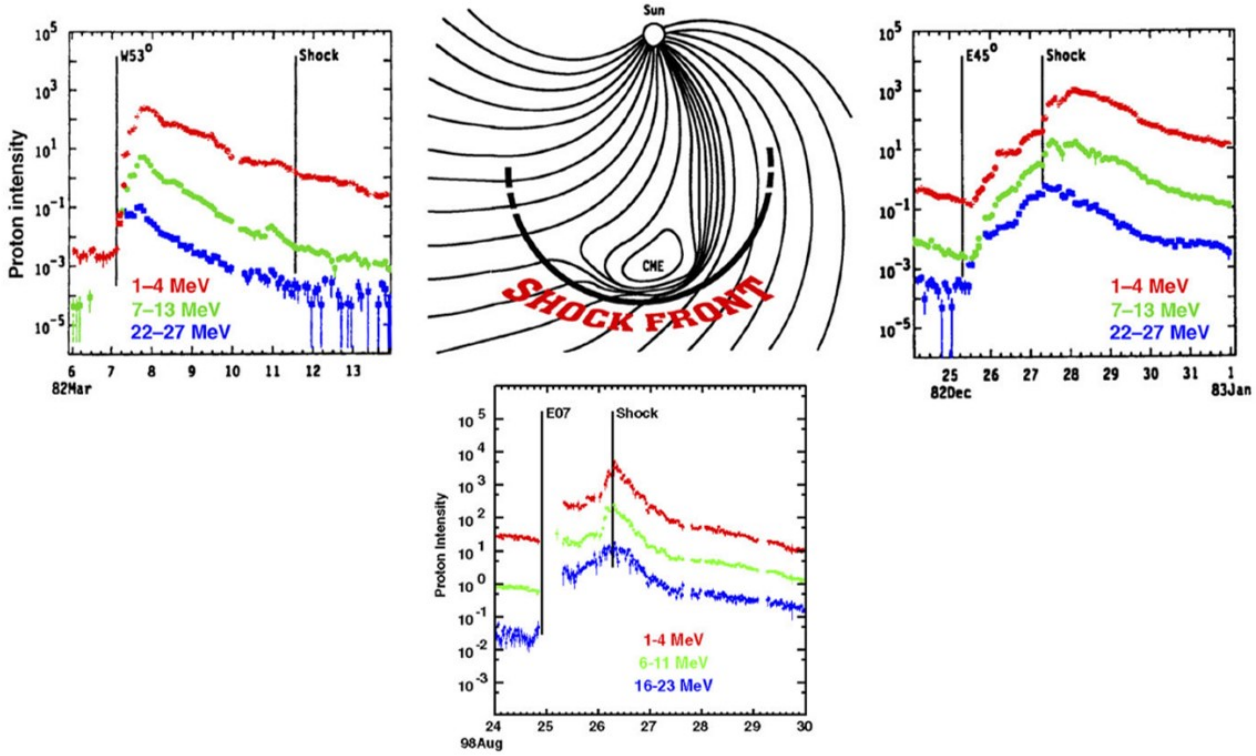

Figure 6: Typical proton intensity time profiles at different solar longitudes obtained from analyses of a large number of gradual SEP events (Cane et al. 1988, Desai & Giacalone 2016).

large scale structure of gradual SEP events by taking measurements at different locations relative to the Sun. Observing at multiple locations allows measurements to be correlated with each other in time, providing distinction between the spatial and temporal behaviour of gradual events which would not be possible if observing from one location alone (Reames, 2013). Intensities measured by *IMP* 8 and *Helios* 1 and 2 are displayed in figure 7 as well as a schematic of their paths through the CME as the CME passes over them (Reames, 2013). *Helios* 1 meets the event near the central meridian, observing the highest intensity as the shock passes, the shock then passes both *Helios* 2 and *IMP* 8 and all three craft enter the particle reservoir. During this time, marked by the interval R, the craft observe near identical intensities independent of location as expected of the reservoir region. Without multiple observing locations, it would be impossible to record this region of invariant intensity.

Measurements can only be taken if a craft is magnetically connected to the SEP source. Thus, in addition to correlating results, having multiple craft taking measurements at the same time, in different locations, increases the degree of magnetic connectivity between observers and the SEP source, meaning more particles are detected from a wider range of locations within the event. Multiple craft also increase the frequency with which measurements can be made and add a form of redundancy if an observing craft is damaged during operation (Hyndman et al., 2024).

A notable multi-craft observation took place in January 1978 when four spacecraft, *Helios* 1 and 2, *IMP* 8 and *Voyager* 2, were used to measure proton intensities, displayed in figure 8, over a large separation. Reames (2023) described this observation as 'fortuitous' because *Voyager* 2 was not originally intended to supplement *Helios*. Each craft played its part in the observation. *Helios* 1 was well-connected to the event central meridian and so

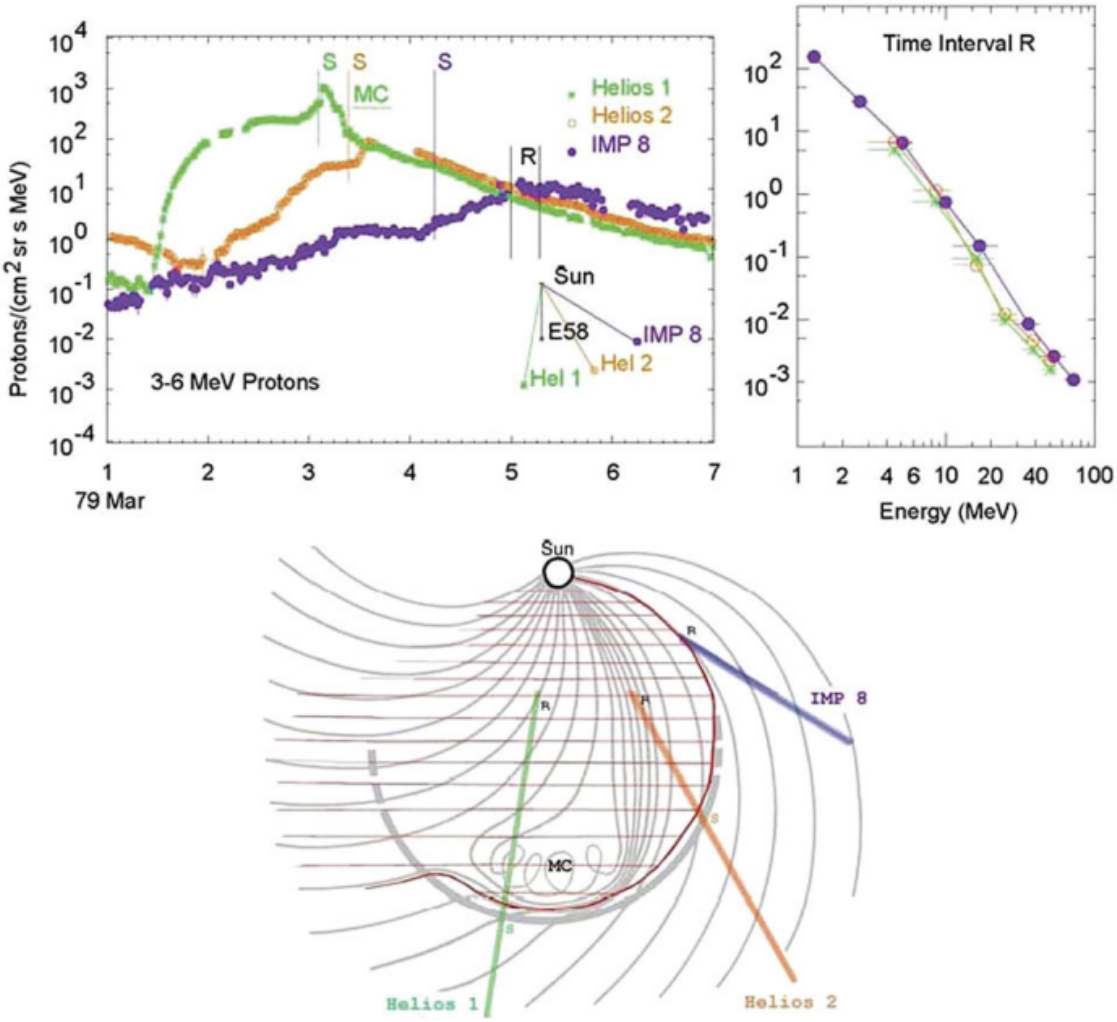

Figure 7: *Upper-left*: Proton intensity-time profiles measured by *IMP* 8 and *Helios* 1 and 2 during a gradual event in early March 1979. Time of shock passage at each craft is denoted S. *Upper-right*: Intensities measured by each craft during the time interval denoted R representing the time at which each craft enters the event reservoir. *Lower*: A schematic detailing the path of each craft through the CME (Reames, 2013).

measured the highest intensities near to the Sun. *Helios* 2 and *IMP* 8 took measurements at around 1 AU documenting the evolution of the event since the shock's encounter with *Helios* 1. *Voyager* 2 then observed the central meridian of the shock as it expanded out to 2 AU. Both *Helios* craft and *IMP* 8 observe the decay phase of the event as *Voyager* 2 encounters the shock front with intensities at *Voyager* 2 decaying to meet those at the others upon shock passage, illustrating the invariance of the particle reservoir.

4.3 Challenges in Space-based Observation

There are various challenges involved in space-based observations of gradual SEP events. Mentioned previously, the large spatial extent of gradual events means observing from a single location is inadequate for producing an accurate representation of the spatial and temporal behaviour of gradual SEP events (Desai & Giacalone 2016, Reames 2013). Multi-craft observations address this issue by providing comparison between observations at various positions.

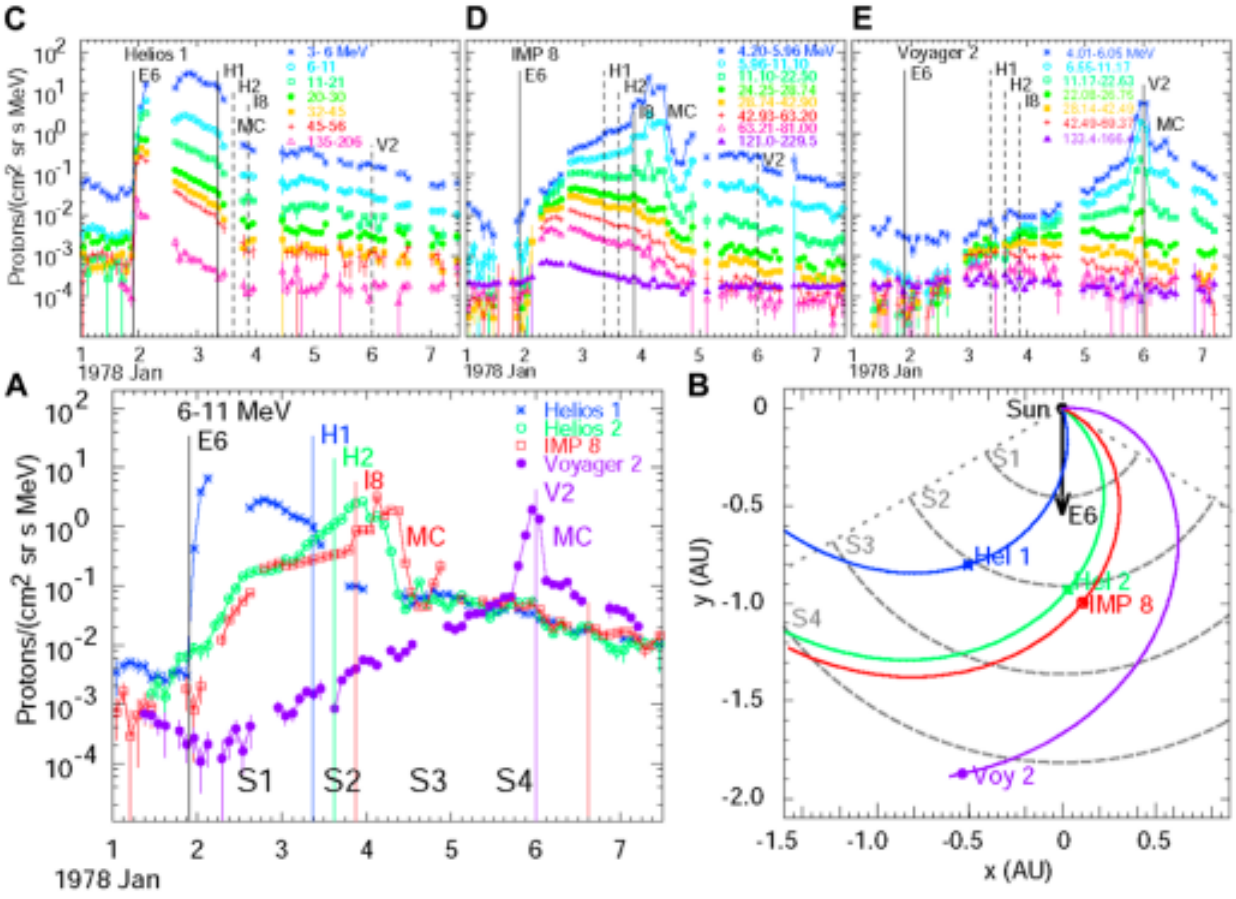

Figure 8: *A*: Proton intensity-time profiles for protons with energies between 6–11 MeV measured by *Helios* 1 and 2, *IMP* 8 and *Voyager* 2 in early January 1978. *B*: A schematic of the initial positions of the four spacecraft detailing their initial magnetic connection to the event. Sequential stages of the shock expansion are marked by dashed grey lines and denoted $S1$, $S2$, $S3$, $S4$. *C*: Intensity profiles in different energy ranges as measured by *Helios* 1. *D*: Intensity profiles in different energy ranges as measured by *IMP* 8. *E*: Intensity profiles in different energy ranges as measured by *Voyager* 2. Event onset time is denoted $E6$ and times of shock passage at each craft are denoted $H1$, $H2$, $I8$ and $V2$, respectively Reames (2023).

Interplanetary scattering can alter the characteristics of detected particles, posing a challenge in gradual event observation. Scattering effects confuse which properties are due to acceleration by the CME shock alone and which are due to scattering during transit, (Desai & Giacalone, 2016). For example, scattering affects particles with lower mass to charge ratios more than those with higher mass to charge ratios altering detector arrival times (Reames, 2021). This corresponds to higher mass to charge ratio species reaching detectors before lower ratio species, resulting in enhancements of the relative abundances of high mass to charge species compared to lower ratio species. These enhancements then decrease as the lower ratio species 'catch up' and arrive at the detector (Desai & Giacalone, 2016). This makes it difficult to distinguish which physical processes are contributing to which properties of an event. Multi-craft observations can also be used to address this issue by taking measurements near the Sun where scattering effects are minimal and comparing them to measurements made further away from the Sun where and when scattering will have had an impact on the evolution of the event (Desai & Giacalone, 2016).

High energy particles incident on spacecraft can cause damage to on-board electronics and spacecraft materials, presenting an obstacle for mission design. Energetic protons and electrons can cause ionisation damage to insulation layers in electronics and lasting damage to solar cells. Particles with enough energy can even cause permanent integrated circuit failure which can be detrimental to instrumentation aboard craft (Fleetwood et al., 2000). To prevent damage to electronics, craft are designed with in-built shielding material, introducing a trade-off between protection and mission cost and feasibility (Fleetwood et al. 2000, Thibeault et al. 2012).

4.4 Recent and Future Developments

Most recently, NASA's *Parker Solar Probe* (*PSP*) has been taking near-Sun measurements of SEPs in an effort to better understand the solar corona. *PSP* was launched in August 2018 and made its closest ever approach of the Sun in late December 2024 with a perihelion of $9.86\,R_{\odot}$ (Raouafi et al., 2023). As the closest man-made object to the Sun, *PSP* skims the solar corona to investigate the coronal structure and how it contributes to SEP events. Instrumentation on-board *PSP* is capable of measuring radio emissions, plasma waves and electric and magnetic fields as well as particle velocity distributions (George et al. 2024, Raouafi et al. 2023). Measurements of these properties in the near-Sun environment will be useful in limiting the effect of interplanetary scattering on observations (Desai & Giacalone, 2016). There are two more solar orbits left in *PSP*s primary mission with the final perihelion of this mission predicted to be in June 2025. Until then, *PSP* will continue to collect date in and around the solar maximum time period, hopefully providing novel results concerning the coronal heating mechanism and how it impacts solar energetic particle events.

In the near future, NASA intends to launch the *Sun Radio Interferometer Space Experiment*, or *SunRISE*. Composed of six CubeSats, *SunRISE* aims to act as a radio interferometer, via aperture synthesis interferometry, to observe low frequency solar radio bursts which can't be observed on Earth due to absorption in the ionosphere at high radio wavelengths (Lazio et al., 2022). *SunRISE* has the capability of imaging and tracking type II radio bursts at frequencies less than 15 MHz to determine how these radio bursts relate to the structure of CME shocks. Notably, the *SunRISE* CubeSats are designed to carry out a small amount of on-board processing with the majority of processing taking place on the ground (Lazio et al., 2022).

5 Conclusion

Gradual SEP events produce the highest particle intensities at Earth, making them an ongoing topic of research due to the radiation hazard they create. Coronal mass ejections moving faster than the local Alfvén speed create a shock wave which accelerates particles as it propagates out into the heliosphere. Acceleration is carried out via diffusive shock acceleration, a resonant process which involves the excitation of a spectrum of Alfvén plasma waves, depending on particle rigidity and local magnetic field strength. Particles are confined to the shock by induced Alfvén waves producing a streaming limit in the intensities of particles streaming away from the shock and a region behind the shock known as a reservoir where intensities are invariant over space and time. The streaming limit and reservoir can be observed in measurements of proton intensities. Alfvén waves scatter particles based on mass to charge ratio with lower mass to charge ratio particles being scattered more efficiently producing trends in relative abundances which can be used to measure plasma source temperature.

Finally, diffusive shock acceleration produces a power law distribution in particle momentum.

Due to the Earth's atmosphere and magnetic field, the majority of gradual event observations are carried out in space. As aforementioned, proton intensities and relative ion abundances can be used to infer gradual event properties such as the streaming limit and reservoir, plasma source temperature and particle origin. Type II radio bursts can be observed on the ground allowing plasma density profiles and shock speeds to be determined. The most energetic gradual events can cause ground level enhancements which can also be observed on the ground using equipment designed for observing cosmic rays. Ground level enhancements can cause changes in Earth's atmosphere and local magnetic field which can be detrimental for satellites, astronauts and electronics on the ground in the most energetic cases.

Space-based observations are central to gradual SEP event research. Key missions such as *Skylab* and *Ulysses* observed important properties of gradual SEP events such as their link to CMEs and invariant reservoir intensities, respectively. Multi-craft observations are used to tackle the challenge posed by the large spatial extent of gradual events for observations at a single location. They do this by allowing correlation of measurements made at multiple locations, decrease the impact of longitude dependence and distinguishing spatial and temporal behaviour. Further, multi-craft observations can be used to quantify the effect that interplanetary scattering has on measurements by comparison of measurements made in a scatter-free environment to those made in an environment where scattering has a bigger impact. Near-Sun missions such as *Parker Solar Probe* aim to take measurements in a scatter-free environment, granting this kind of comparison. The planned future mission *SunRISE* shows promise for being able to measure low frequency solar radio bursts, imaging and tracking these bursts to better understand CME shock structure.

References

Bastian, T. S., Benz, A. O., & Gary, D. E. 1998, Annual Review of Astronomy and Astrophysics, 36, 131, doi: 10.1146/annurev.astro.36.1.131

Boteler, D. H. 2019, Space Weather, 17, 1427, doi: 10.1029/2019SW002278

Bothmer, V., Posner, A., Kunow, H., et al. 1997. https://www.semanticscholar.org/paper/Solar-energetic-particle-events-and-coronal-mass-Bothmer-Posner/f9607aec94c001608aafae08b945ae3e99d8cd18

Bougeret, J. L., Kaiser, M. L., Kellogg, P. J., et al. 1995, Space Science Reviews, 71, 231, doi: 10.1007/BF00751331

Cane, H. V., Reames, D. V., & von Rosenvinge, T. T. 1988, Journal of Geophysical Research, 93, 9555, doi: 10.1029/JA093iA09p09555

Chen, P. F. 2011, Living Reviews in Solar Physics, 8, 1, doi: 10.12942/lrsp-2011-1

Cliver, E. W. 2008, Proceedings of the International Astronomical Union, 4, 401, doi: 10.1017/S1743921309029639

Cristofari, P., Blasi, P., & Caprioli, D. 2022, The Astrophysical Journal, 930, 28, doi: 10.3847/1538-4357/ac6182

Cucinotta, F. A., Hu, S., Schwadron, N. A., et al. 2010, Space Weather, 8, doi: 10.1029/2010SW000572

Cucinotta, F. A., Schimmerling, W., Blakely, E. A., & Hei, T. K. 2021, Life Sciences in Space Research, 31, 59, doi: 10.1016/j.lssr.2021.07.005

Desai, M., & Giacalone, J. 2016, Living Reviews in Solar Physics, 13, 3, doi: 10.1007/s41116-016-0002-5

Drury, L. O. 1983, Reports on Progress in Physics, 46, 973, doi: 10.1088/0034-4885/46/8/002

Fleetwood, D. M., Winokur, P. S., & Dodd, P. E. 2000, Microelectronics Reliability, 40, 17, doi: 10.1016/S0026-2714(99)00225-5

Forbush, S. E. 1946, Physical Review, 70, 771, doi: 10.1103/PhysRev.70.771

George, H., Malaspina, D. M., Lee-Bellows, D., et al. 2024, Astronomy & Astrophysics, 689, A214, doi: 10.1051/0004-6361/202450244

Gonzalez, W. D., Joselyn, J. A., Kamide, Y., et al. 1994, Journal of Geophysical Research: Space Physics, 99, 5771, doi: 10.1029/93JA02867

Gopalswamy, N., Mäkelä, P., & Yashiro, S. 2019, A Catalog of Type II Radio Bursts Observed by Wind/WAVES and their Statistical Properties, arXiv, doi: 10.48550/arXiv.1912.07370

Gopalswamy, N., Xie, H., Yashiro, S., et al. 2012, Space Science Reviews, 171, 23, doi: 10.1007/s11214-012-9890-4

Gosling, J. T. 1993, Journal of Geophysical Research: Space Physics, 98, 18937, doi: 10.1029/93JA01896

Hyndman, R. A., Dalla, S., Laitinen, T., et al. 2024, Multi-spacecraft observations of the decay phase of solar energetic particle events, arXiv. http://arxiv.org/abs/2411.07903

Iucci, N., Levitin, A. E., Belov, A. V., et al. 2005, Space Weather, 3, doi: 10.1029/2003SW000056

Kahler, S. W. 2001, Journal of Geophysical Research: Space Physics, 106, 20947, doi: 10.1029/2000JA002231

Kahler, S. W., Tylka, A. J., & Reames, D. V. 2009, The Astrophysical Journal, 701, 561, doi: 10.1088/0004-637X/701/1/561

Kim, K.-H., Kim, G.-J., & Kwon, H.-J. 2018, Earth, Planets and Space, 70, 174, doi: 10.1186/s40623-018-0947-9

Kim, M.-H. Y., De Angelis, G., & Cucinotta, F. A. 2011, Acta Astronautica, 68, 747, doi: 10.1016/j.actaastro.2010.08.035

Kumari, A., Morosan, D. E., Kilpua, E. K. J., & Daei, F. 2023, Astronomy & Astrophysics, 675, A102, doi: 10.1051/0004-6361/202244015

Laming, J. M. 2009, The Astrophysical Journal, 695, 954, doi: 10.1088/0004-637X/695/2/954

Lazio, J., Kasper, J. C., Romero-Wolf, A., Lux, J. P., & Neilsen, T. L. 2022 (AGU). https://agu.confex.com/agu/fm22/meetingapp.cgi/Paper/1078515

Melrose, D. B. 2017, Reviews of Modern Plasma Physics, 1, 5, doi: 10.1007/s41614-017-0007-0

Ng, C. K., Reames, D. V., & Tylka, A. J. 1999, Geophysical Research Letters, 26, 2145, doi: 10.1029/1999GL900459

Raouafi, N. E., Matteini, L., Squire, J., et al. 2023, Space Science Reviews, 219, 8, doi: 10.1007/s11214-023-00952-4

Reames, D. V. 1999, Space Science Reviews, 90, 413, doi: 10.1023/A:1005105831781

—. 2002, Space Radiation (Japan). https://epact2.gsfc.nasa.gov/don/02SEP.pdf

—. 2004, Advances in Space Research, 34, 381, doi: 10.1016/j.asr.2003.02.046

—. 2013, Space Science Reviews, 175, 53, doi: 10.1007/s11214-013-9958-9

—. 2016, Solar Physics, 291, 911, doi: 10.1007/s11207-016-0854-9

—. 2021, Lecture Notes in Physics, Vol. 978, Solar Energetic Particles: A Modern Primer on Understanding Sources, Acceleration and Propagation (Cham: Springer International Publishing), doi: 10.1007/978-3-030-66402-2

—. 2023, Frontiers in Astronomy and Space Sciences, 10, doi: 10.3389/fspas.2023.1254266

Reid, H. A. S. 2011, PhD, University of Glasgow. https://eleanor.lib.gla.ac.uk/record=b2857025

Stassinopoulos, E. G., & LaBel, K. A. 2004, The Near-Earth Space Radiation for Electronics Environment. https://ntrs.nasa.gov/citations/20040171273

Thibeault, S. A., Fay, C. C., Lowther, S. E., et al. 2012, Radiation Shielding Materials Containing Hydrogen, Boron, and Nitrogen: Systematic Computational and Experimental Study. https://ntrs.nasa.gov/citations/20160010096

Tylka, A. J., Cohen, C. M. S., Dietrich, W. F., et al. 2001, The Astrophysical Journal, 558, L59, doi: 10.1086/323344

Usoskin, I. G., Kovaltsov, G. A., Mironova, I. A., Tylka, A. J., & Dietrich, W. F. 2011, Atmospheric Chemistry and Physics, 11, 1979, doi: 10.5194/acp-11-1979-2011

Whitman, K., Egeland, R., Richardson, I. G., et al. 2023, Advances in Space Research, 72, 5161, doi: 10.1016/j.asr.2022.08.006

Wild, J. P., & McCready, L. L. 1950, Australian Journal of Scientific Research A Physical Sciences, 3, 387, doi: 10.1071/CH9500387